Available online at www.sciencedirect.com

SCIENCE DIRECT

Genomics 85 (2005) 273–279

GENOMICS

www.elsevier.com/locate/ygeno

Short Communication

Uncommon *Alu*-mediated NF1 microdeletion with a breakpoint inside the *NF1* gene

Cristina Gervasini[a], Marco Venturin[a], Francesca Orzan[a], Alessandra Friso[b], Maurizio Clementi[b], Romano Tenconi[b], Lidia Larizza[a], Paola Riva[a,*]

[a]*Department of Biology and Genetics, Medical Faculty, University of Milan, via Viotti 3/5, 20133 Milan, Italy*
[b]*Clinical Genetics and Epidemiology Unit, Department of Pediatrics, University of Padua, Padua, Italy*

Received 22 July 2004; accepted 23 October 2004

Abstract

Neurofibromatosis type 1 (NF1) microdeletion syndrome is caused by haploinsufficiency of the *NF1* gene and of gene(s) located in adjacent flanking regions. Most of the *NF1* deletions originate by nonallelic homologous recombination between repeated sequences (REP-P and -M) mapped to 17q11.2, while a few uncommon deletions show unusual breakpoints. We characterized an uncommon 1.5-Mb deletion of an NF1 patient displaying a mild phenotype. We applied high-resolution FISH analysis allowing us to obtain the sequence of the first junction fragment of an uncommon deletion showing the telomeric breakpoint inside the IVS23a of the *NF1* gene. Sequence analysis of the centromeric and telomeric boundaries revealed that the breakpoints were present in the AluJb and AluSx regions, respectively, showing 85% homology. The centromeric breakpoint is localized inside a χ-like element; a few copies of this sequence are also located very close to both breakpoints. The in silico analysis of the breakpoint intervals, aimed at identifying consensus sequences of several motifs usually involved in deletions and translocations, suggests that *Alu* sequences, probably associated with the χ-like element, might be the only recombinogenic motif directly mediating this large deletion.

Keywords: Uncommon NF1 microdeletion; Breakpoint junction; *Alu* sequences; χ-like element

It is well known that neurofibromatosis type 1 (NF1; MIM +162200) is a common autosomal dominant condition affecting 1/3500 individuals and that approximately 5–20% of all NF1 patients carry a heterozygous deletion involving the *NF1* gene and the contiguous genes underlying the so-called "NF1 microdeletion syndrome" [1,2].

Like other genomic disorders, NF1 deletions are mediated by specific architectural genomic features that account for the common occurrence of standard-sized deletions [3], although different deletion endpoints and sizes have been identified in a subset of patients [1–7]. The majority (80%) of microdeletions display an ~1.4-Mb size with breakpoints clustered at paralogous sequences flanking the *NF1* gene called NF1-REP-P (proximal) and NF1-REP-M (medial) [3,4]. The REP-mediated deletions probably occur as a result of interchromosomal recombination of misaligned NF1-REP elements or intrachromosomal looping-out [2,3]. A second type of recurrent NF1 deletion, mediated by intrachromosomal recombination between the *JJAZ1* gene and its pseudogene, has been recently described [4,6,7].

Most of the sequence deletion breakpoints, localized within the NF1-REP-P and -M or in the *JJAZ1* gene/pseudogene, are mediated by nonallelic homologous recombination (NAHR) [7–9]. Only one case of atypical deletion non-LCR mediated with a sequenced breakpoint junction has been reported [4], and the underlying mechanism has been found to be nonhomologous end-joining [8,9].

Following allelic segregation analysis, the patient here described showed uninformative *NF1* polymorphic markers

* Corresponding author. Fax: +39 02 50315864.
E-mail address: paola.riva@unimi.it (P. Riva).

0888-7543/$ - see front matter © 2004 Elsevier Inc. All rights reserved.
doi:10.1016/j.ygeno.2004.10.014

until the IVS27 microsatellite, which was shown to be heterozygous, and the remaining markers mapped to the 3′ end of the gene. To establish whether a NF1 deletion was present, we performed FISH studies with BAC 23O13, specific for *NF1*, that showed decreased signals on one chromosome 17, mapping the telomeric deletion boundary in the *NF1* gene. To define the proximal deletion breakpoint, we applied FISH analysis to a set of clones centromeric to *NF1:* the centromeric breakpoint was mapped to BAC 68I3, showing a decreased signal. All the clones covering the 1.5-Mb region between 23O13 and 68I3 were deleted, with the exception of the NF1-REP-specific clone 271K11, which showed a decreased signal on one chromosome due to the deletion of REP-P and the presence of REP-M. We verified and showed the contiguity of the clones 23O13 and 68I3 by FISH on DNA fibers from the patient (Fig. 1a).

To refine the critical breakpoint regions, we generated from the 68I3 and 23O13 clones 20 locus-specific FISH probes by long-range and *Alu* PCR [10]. We mapped by FISH the centromeric deletion breakpoint to a 7-kb interval, between the 68c and the 68d probes, which were observed to be not deleted and deleted, respectively (Figs. 1b and 1c). As far as the telomeric breakpoint, we found in replicated experiments that none of the *NF1* locus-specific probes showed a complete deletion on one chromosome 17. From 23a (exon 1) to 23i (exon 22) we detected decreased signals, while from 23l (exon 24) to 23o (intron 27b) all the probes showed similar signals on both chromosomes (Figs. 1b and 1c). Probing the Centaurin α2 gene, which is located 136 kb upstream of the *NF1* gene, a complete lack of FISH signals was recorded (Figs. 1b and 1c).

A possible explanation for the observed decreased intensity of the *NF1*-specific signals is the deletion of a portion of the *NF1* gene combined with cross-hybridization of *NF1* homologous sequences not included in the deletion. This finding is commonly observed when NF1-REP-specific clones are used, being peculiar to all duplicated sequences. Thus, we localized the telomeric breakpoint to an interval of 8 kb, between probes 23i and 23l (Fig. 1c).

Based on these findings we developed a set of eight primers within the centromeric and telomeric intervals previously identified, to isolate and sequence the breakpoint junction. By using different primer combinations, we performed long-range PCR on genomic DNA from the patient and several controls and obtained a fragment of 6 kb

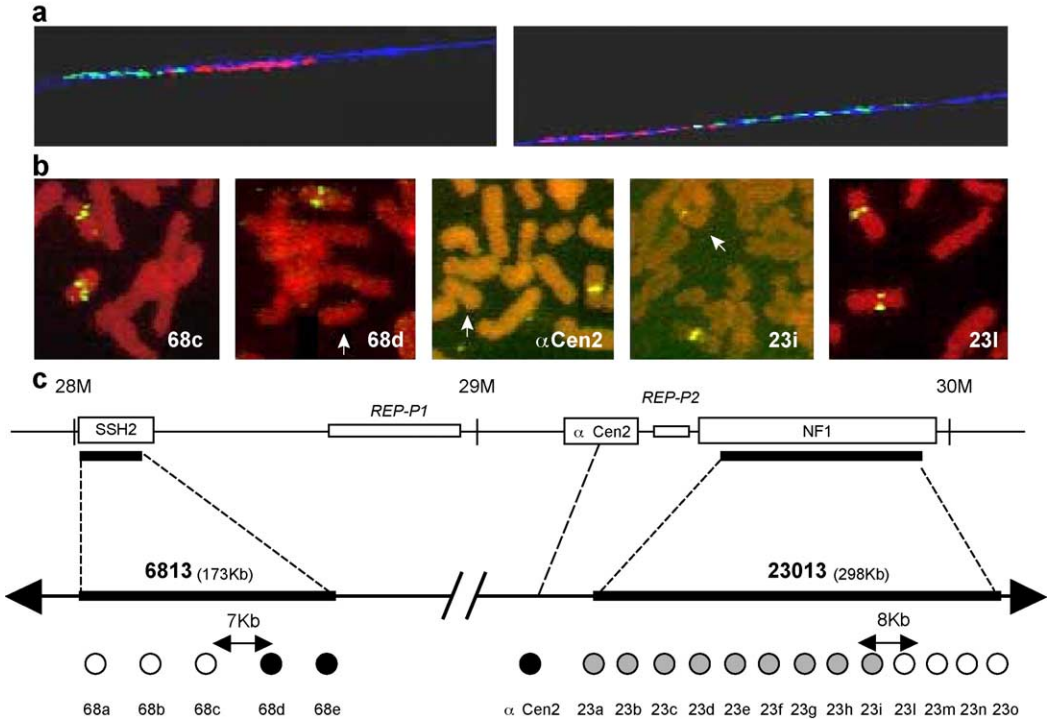

Fig. 1. (a) Fiber-FISH with clones 68I3 (green) and 23O13 (red) showing partially overlapping red and green signals encompassing the breakpoint regions. (b) FISH on metaphases from patient with locus-specific probes mapping to the centromeric and telomeric breakpoint regions. The centromeric probes 68c and 68d show two and one 17-specific signal, respectively. The telomeric probes 23i (as 23a–23h) show one decreased signal, whereas 23l shows two signals. The probe αCen, 135 kb upstream the *NF1* gene, shows one signal on the non deleted chromosome. The deleted chromosomes 17 are indicated by arrows. (c) Summary of the results of FISH experiments using locus-specific probes. The top shows a schematic map of the *NF1* region and the REP-P (white box) and the genomic clones targeting the breakpoint regions at their native positions on chromosome 17. A magnification of the clones at the deletion boundaries is provided at the bottom, the clone-generated locus-specific probes being shown below as circles. The black circles are for deleted probes, the gray circles for probes showing a decreased signal on the deleted chromosome, and the open circles for nondeleted probes. The sizes of the intervals delimited by the deleted and the flanking nondeleted probes comprising the breakpoints are also indicated by the double arrows.

only in the patient's DNA. The sequencing of the junction fragment (Fig. 2a) revealed a perfect alignment with the sequence of centromeric and telomeric regions adjacent to the breakpoints (Fig. 2b).

By this characterization we could map the telomeric breakpoint within *NF1* IVS23a and the centromeric breakpoint within *SSH2* (sling-shot homologous 2) IVS4, calculating a deletion extent of 1563 kb. Due to the opposite transcription directions of *NF1* and *SSH2*, a chimeric SSH2–NF1 transcript is not expected.

The analysis of the genomic intervals containing the centromeric and telomeric boundaries revealed that the breakpoints are present in AluJb and AluSx sequences, respectively (Fig. 2c), showing 85% homology in the stretch of 115 bp around the breakpoint junction. In addition, an AluSx is present 50 bp downstream of the centromeric

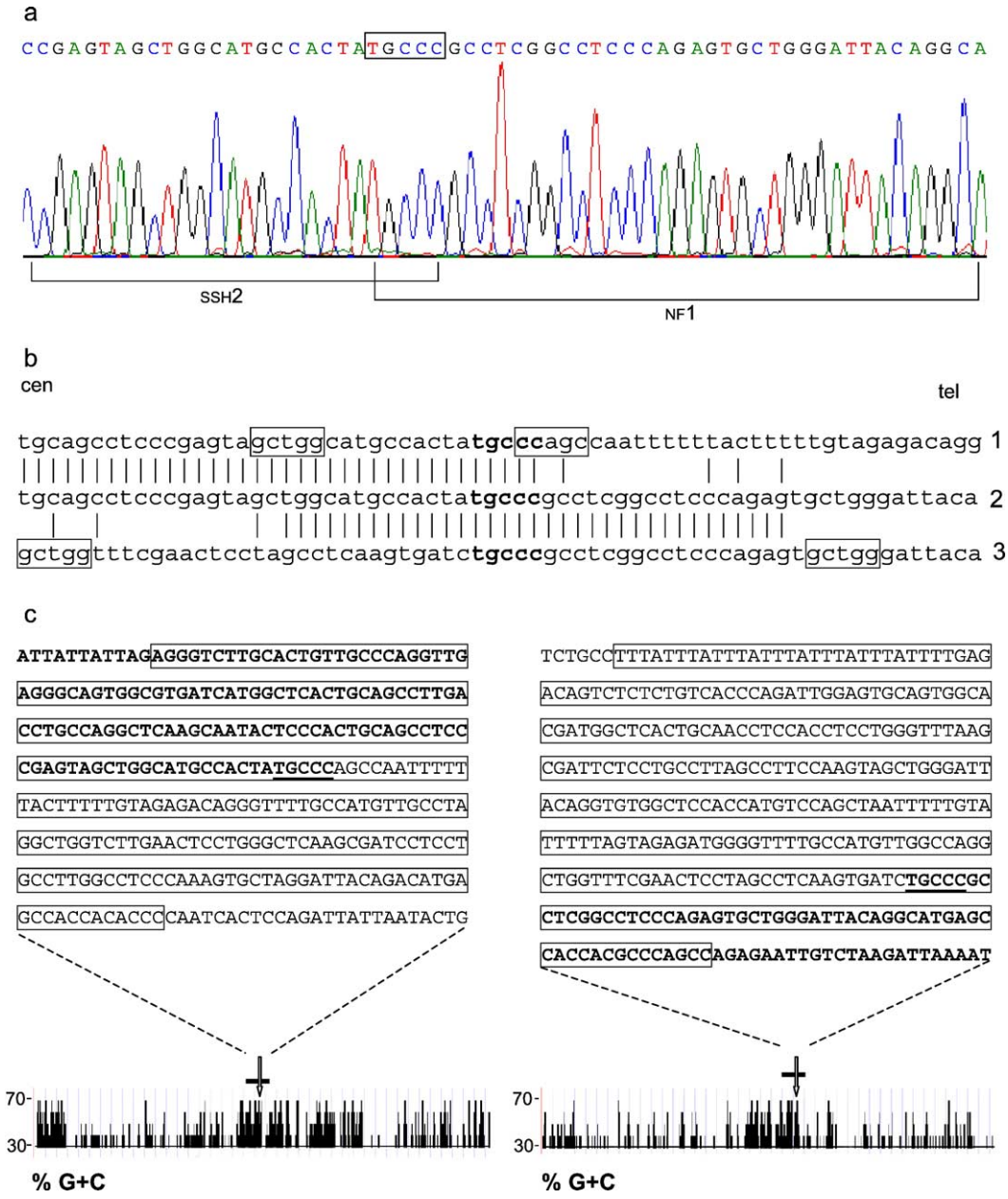

Fig. 2. (a) Electropherogram of the sequence showing the junction between *SSH2* and *NF1*. (b) Sequence from centromere to telomere of patient deletion junction fragment (line 2). Sequences derived from the centromeric and telomeric endpoints of the deletion are indicated by lines 1 and 3, respectively. The stretch "tgccc," in bold, is localized on the junction, in both the centromeric and the telomeric sequence. The stretch corresponds to bases 2350–2354 of the IVS4 of the *SSH2* gene (end of centromeric BKP) and to bases 7262–7266 of the IVS23a of the *NF1* gene (end of telomeric BKP). Boxes frame the core of the χ-like elements, present in the centromeric and telomeric breakpoint regions. (c) Normal sequence of the centromeric (left) and telomeric (right) breakpoint regions. The breakpoint is localized at the border between normal and boldface (stretch "TGCCC," underlined). Boxes indicate *Alu* sequences. G + C percentages of the 2.5-kb regions around the breakpoints are displayed using the graphic output from UCSC Genome Bioinformatics (http://genome.ucsc.edu/). The picks indicated by arrows coincide with the breakpoints.

AluJb motif, while 30 bp upstream the MER5 and L2 motifs, all showing 100% homology with the AluSx targeting the telomeric breakpoint, were detected.

Interestingly, the centromeric breakpoint is localized into the internal element of a χ-like sequence (GCTGG). Additional copies of this element and its reverse complement (CCAGC) are located very close to both breakpoints (Fig. 2b). The χ element, a mediator of prokaryotic recombination, represented by 26 bp of the core region of some *Alu* sequences [11], was observed in the proximity of the breakpoint of reported *Alu*-mediated deletions [12–15]. In addition, the junction sequence was screened in silico for the presence of DNA sequence motifs shown to be associated with site-specific recombination and rearrangements [16], including topoisomerase cleavage sites, translin target sites, human minisatellites, immunoglobulin heavy-chain class switch sites, DNA polymerase pause and frameshift hot spots (MAR-Wiz, http://futuresoft.org), palindromes (Palindrome, http://bioweb.pasteur.fr/seqanal/interfaces/palindrome), and promoter sequences (First Exon Finder, http://rulai.cshl.org/tools/FirtsEF/). None of these motifs was detected at breakpoint boundaries of the patient deletion in agreement with Abeysinghe et al. [16], who found that these motifs are more represented at translocation than at deletion breakpoints, with the exception of *Alu* sequences and χ elements. Both the centromeric and the telomeric breakpoints coincide with a pick of 70% in the G + C content, a percentage significantly higher compared to the surrounding sequences, indicating that the breakpoints map in regions known as hot spots for meiotic recombination [17] (Fig. 2c).

The deletion here studied is so far one of the largest mediated by *Alu* sequences, while these types of deletions usually range from a few to 200 kb [14,15,18–22]. The uncommon deletions in the 4-Mb Smith–Magenis syndrome region were recently found to present *Alu* sequences in the breakpoint region, but in an LCR context [23]. Unlike the similar-sized NF1-REP deletions, which are based on the NAHR mechanism, the atypical NF1 deletion here characterized seems to have been *Alu*-mediated. The finding that a 1.5-Mb deletion is mediated by *Alu* sequences might be accounted for by the presence of χ elements in the *Alu* stretches involved in the breakpoints and by the location of a centromeric breakpoint in an *Alu*-rich region (Figs. 2b and 2c). In addition, the peculiar genomic structure of the LCR-rich 17q11.2 region [3,24] might stimulate, but not mediate directly, the recombination event [9], acting synergistically with *Alu* sequences.

The genetic analysis of patients affected by NF1 evidenced the direct involvement of the *NF1* gene in several rearrangements, such as large intragenic deletions and translocations [25–30], but peculiar to this case is that a deletion with an extent of more than 1 Mb has one breakpoint located within the *NF1* gene. With regard to breakpoint localization within the *NF1* gene, IVS31 was reported to be involved in both an intragenic deletion [28] and a translocation [31,32], while in a region comprising the exon 23-2 and exon 24 cluster the breakpoints of an intragenic deletion [26], a translocation [33], and the centromeric deletion end are here reported. Interestingly, one of the first mutations affecting the *NF1* gene was the insertion of an *Alu* element arising by retrotransposition [34], a finding attesting to the recombinogenic nature of these interspersed repetitive sequences.

Further allelic segregation studies of *NF1* 5′ extragenic polymorphisms showed the paternal derivation of the deletion. The lack of the novel junction deletion fragment following PCR of paternal DNA demonstrated that the deletion occurred de novo in the proband. Unfortunately, we could not establish whether an intrachromosomal or interchromosomal recombination occurred as the allelic segregation analysis could not have been extended to the grandparents.

The detection by FISH of residual fluorescent *NF1*-specific signals on the deleted chromosome 17 using probes targeting the region upstream of the telomeric breakpoint is consistent with the presence of additional *NF1*-like sequences, similar to the deleted *NF1* portion. While the existence of *NF1* duplicated sequences in the 17q11.2 region is an open question [35,36], the evidence obtained from the deleted chromosome of the patient indicates that duplicated *NF1* sequences might have been present before the generation of the deletion or might have resulted from a complex rearrangement leading to the deletion/duplication; which of these possibilities is true is not possible to know.

As far as the phenotype, patients with large deletions often show, in addition to the classical NF1 signs contained in the NIH Consensus Criteria, dysmorphisms, mental retardation, cardiac anomalies, and malignant peripheral nerve sheath tumors [36,37]. The patient analyzed, an 8-year-old male, the only child of nonconsanguineous healthy parents, was evaluated regularly for growth using the NF1 growth charts [38]. He shows several cafè-au-lait spots, axillary and inguinal freckling, one typical Lisch nodule of the right iris, and nonprogressive optic glioma. Several febrile and nonfebrile seizures required continuous anticonvulsant therapy. The DQ (Standford–Binet test) at the age of 4 years was borderline. The absence of mental retardation, dysmorphisms, and cardiac anomalies, which are the most represented extra NF1 clinical signs in microdeleted patients [37], seems to indicate that these phenotypes may be caused by haploinsufficiency of genes mapping downstream of the *NF1* gene, even if additional similar cases are needed to confirm this hypothesis.

This study, reporting the first case of a 1.5-Mb NF1 deletion with an *NF1* intragenic breakpoint, evidenced, as the only recombinogenic motif, an *Alu* sequence associated with the χ-like element, reinforcing the crucial role of these structures in the rearrangement leading to large deletions. This evidence agrees with one of the mechanisms that have recently been postulated for atypical Smith–Magenis dele-

tions, but in our patient this mechanism, i.e., *Alu*-mediated recombination, seems to act singly [23].

The described patient can be considered a paradigmatic case for further studies on genomic structure of the 17q11.2 region and mapping of *NF1* intragenic sequences possibly involved in complex rearrangements.

Materials and methods

Preparation of clones

All of the PAC and BAC clones were supplied by the DIBIT-HSR Resource Center (Milan, Italy) or purchased from the CHORI BACPAC Resource Center (Oakland, CA, USA). DNA was obtained starting from a single colony grown in 4 ml of LB medium supplemented with 25 μg/ml kanamycin (Sigma) for PACs and 20 μg/ml chloramphenicol (Sigma) for BACs following standard procedures.

Locus-specific probe preparation

The method previously described [10] is based on two consecutive reactions using PAC and BAC clones containing the loci of interest.

Cell cultures and chromosome preparation

A lymphoblastoid cell line from the patient was established from peripheral blood using Epstein–Barr virus according to standard procedures, by means of a service provided by the Biochemical and Genetics Lab of Neurological Institute C. Besta in Milan. The cell culture was performed by standard protocols. The chromosome preparations were obtained using a standard technique.

Preparation of stretched chromosomes and DNA fibers

The chromosomes were stretched mechanically as previously described [39]. The fiber slides were prepared using a previously described procedure [40].

FISH

BAC and PAC clones and locus-specific probes were labeled with digoxigenin–dUTP and biotin–dUTP (Roche Diagnostic) using a nick-translation kit (Roche Diagnostic). The FISH experiments were performed according to standard procedures [41]. The detection protocol included a three layer fluorescein–streptavidin anti-avidin system (Sigma) for the biotin-labeled probes and a Cy3–anti-digoxigenin conjugated antibody (Jackson ImmunoResearch Laboratories) for the digoxigenin-labeled probes. The chromosomes and fiber were counterstained with propidium iodide and DAPI in antifade (Vectashield) and then visualized using a Leitz DM-RB microscope equipped for DAPI and FITC/TRITC epifluorescence optics. The images were captured by means of a CCD camera (Hamamatsu 3CCD camera, C5810) and visualized using Highfish software (Casti Imaging).

Deletion-junction fragment and sequence analysis

The deletion-junction fragment analyses were performed using the Expand Long Template PCR System (Roche Molecular Biochemicals) according to the manufacturer's instructions using primer Fw, 5′-CTATCAAACTTT-TAACCTTCTGC-3′, and Rev, 5′-ACCTTCTGGGGAC-GAGGAACC-3′. PCR products were sequenced directly by using the Big Dye Terminator kit (Applied Biosystem) and resolved on a 3100 ABI Prism genetic analyzer (Applied Biosystem).

Sequence in silico analysis

The in silico sequence analysis was performed using the following database and bioinformatic tools: Entrez Nucleotides Database, http://www.ncbi.nlm.nih.gov/Entrez/query.fcgi?db=nucleotide; MAR-Wiz, http://www.futuresoft.org/ (for searching recombination-specific sites); First Exon Finder, http://rulai.cshl.org/tools/FirtsEF/ (for searching promoter sequences); NCBI BLAST, http://www.ncbi.nlm.nih.gov/Blast/; UCSC Genome Bioinformatics, http://www.genome.ucsc.edu/ (for the sequence homology analyses and analysis of the BAC/PAC clones used as probes in the FISH experiments and as templates in locus-specific probe preparation and for the G + C content); and Palindrome, http://bioweb.pasteur.fr/seqanal/interfaces/palindrome.htlm (for searching palindromic elements).

Acknowledgments

This work was supported by a 2003 grant from FIRST to P.R. and by a 2002 grant from AIRC to L.L.

References

[1] P. Riva, L. Corrado, F. Natacci, P. Castorina, B.L. Wu, G.H. Schneider, M. Clementi, R. Tenconi, B.R. Korf, L. Larizza, *NF1* microdeletion syndrome: refined fish characterization of sporadic and familial deletions with locus-specific probe, Am. J. Hum. Genet. 66 (2000) 100–109.

[2] D.E. Jenne, S. Tinschert, H. Reimann, W. Lasinger, G. Thiel, H. Hameister, H. Kehrer-Sawatzki, Molecular characterization and gene content of breakpoint boundaries in patients with neurofibromatosis type 1 with 17q11.2 microdeletions, Am. J. Hum. Genet. 69 (2001) 516–527.

[3] M.O. Dorschner, V.P. Sybert, M. Weaver, B.A. Pletcher, K. Stephens, *NF1* microdeletion breakpoints are clustered at flanking repetitive sequences, Hum. Mol. Genet. 9 (2000) 35–46.

[4] M. Venturin, C. Gervasini, F. Orzan, A. Bentivegna, L. Corrado, P. Colapietro, A. Friso, R. Tenconi, M. Upadhyaya, L. Larizza, P. Riva, Evidence for non-homologous end joining and non-allelic homologous recombination in atypical NF1 microdeletions, Hum. Genet. 115 (2004) 69–80.

[5] H. Kehrer-Sawatzki, S. Tinschert, D.E. Jenne, Heterogeneity of breakpoints in non-LCR-mediated large constitutional deletions of the 17q11.2 NF1 tumor suppressor region, J. Med. Genet. 40 (2003) e116.

[6] E. Petek, D.E. Jenne, J. Smolle, B. Binder, W. Lasinger, C. Windpassinger, K. Wagner, P.M. Kroisel, H. Kehrer-Sawatzki, Mitotic recombination mediated by the *JJAZF1* (KIAA0160) gene causing somatic mosaicism and a new type of constitutional *NF1* microdeletion in two children of a mosaic female with only few manifestations, J. Med. Genet. 40 (2003) 520–525.

[7] H. Kehrer-Sawatzki, L. Kluwe, C. Sandig, M. Kohn, K. Wimmer, U. Krammer, A. Peyrl, D.E. Jenne, I. Hansmann, V.F. Mautner, High frequency of mosaicism among patients with neurofibromatosis type 1 (NF1) with microdeletions caused by somatic recombination of the JJAZ1 gene, Am. J. Hum. Genet. 75 (2004) 410–423.

[8] K. Inoue, D. Osaka, V.C. Thurston, J.T.R. Clarke, A. Yoneyama, L. Rosenbark, T.D. Bird, M.E. Hodes, L.G. Shaffer, J.R. Lupski, Genomic rearrangements resulting in *PLP1* deletion occur by nonhomologous end joining and cause different dysmyelinating phenotypes in males and females, Am. J. Hum. Genet. 71 (2002) 838–853.

[9] P. Stankiewicz, C.J. Shaw, J.D. Dapper, K. Wakui, L.G. Shaffer, M. Withers, L. Elizondo, S.D. Park, JR. Lupski, Genome architecture catalyzes non recurrent chromosomal rearrangements, Am. J. Hum. Genet. 72 (2003) 1101–11016.

[10] P. Riva, L. Corrado, P. Colapietro, L. Larizza, A rapid and simple method of generating locus-specific probes for FISH analysis, Technical Tips Online (http://tto.trends.com) T01618 1999.

[11] N.S. Rudiger, N. Gregersen, M.C. Kielland-Brandt, One short well conserved region of Alu-sequences is involved in human gene rearrangements and has homology with prokaryotic chi, Nucleic Acids Res. 23 (1995) 256–260.

[12] T. Harada, J. Nagayama, K. Kohno, L.A. Mickley, T. Fojo, M. Kuwano, M. Wada, Alu-associated interstitial deletions and chromosomal re-arrangement in 2 human multidrug-resistant cell lines, Int. J. Cancer 86 (2000) 506–511.

[13] K.L. Harteveld, M. Losekoot, R. Fodde, P.C. Giordano, L.F. Bernini, The involvement of Alu repeats in recombination events at the alpha-globin gene cluster: characterization of two alphazero-thalassaemia deletion breakpoints, Hum. Genet. 99 (1997) 528–534.

[14] F. Laccone, I. Junemann, S. Whatley, R. Morgan, R. Butler, P. Huppke, D. Ravine, Large deletions of the MECP2 gene detected by gene dosage analysis in patients with Rett syndrome, Hum. Mutat. 23 (2004) 234–244.

[15] M.I. Lutskiy, L.N. Jones, F.S. Rosen, E. Remold-O'Donnell, An Alu-mediated deletion at Xp11.23 leading to Wiskott–Aldrich syndrome, Hum. Genet. 110 (2002) 515–519.

[16] S.S. Abeysinghe, N. Chuzhanova, M. Krawczak, E.V. Ball, D.N. Cooper, Translocation and gross deletion breakpoints in human inherited disease and cancer. I. Nucleotide composition and recombination-associated motifs, Hum. Mutat. 22 (2003) 229–244.

[17] MW. Nachman, Variation in recombination rate across the genome: evidence and implication, Curr. Opin. Genet. Dev. 12 (2002) 657–663.

[18] M. Botto, K.Y. Fong, A.K. So, R. Barlow, R. Routier, B.J. Morley, M.J. Walport, Homozygous hereditary C3 deficiency due to a partial gene deletion, Proc. Natl. Acad. Sci. USA 89 (1992) 4957–4961.

[19] J.J. Chae, Y.B. Park, S.H. Kim, S.S. Hong, G.J. Song, K.H. Han, Y. Namkoong, H.S. Kim, C.C. Lee, Two partial deletion mutations involving the same Alu sequence within intron 8 of the LDL receptor gene in Korean patients with familial hypercholesterolemia, Hum. Genet. 99 (1997) 155–163.

[20] J. Flint, J. Rochette, C.F. Craddock, C. Dode, B. Vignes, S.W. Horsley, L. Kearney, V.J. Buckle, H. Ayyub, D.R. Higgs, Chromosomal stabilisation by a subtelomeric rearrangement involving two closely related Alu elements, Hum Mol Genet 5 (1996) 1163–1169.

[21] S. Gad, I. Bieche, M. Barrois, F. Casilli, S. Pages-Berhouet, C. Dehainault, M. Gauthier-Villars, A. Bensimon, A. Aurias, R. Lidereau, B. Bressac-de Paillerets, M. Tosi, S. Mazoyer, D. Stoppa-Lyonnet, Characterisation of a 161 kb deletion extending from the NBR1 to the BRCA1 genes in a French breast–ovarian cancer family, Hum. Mutat. 21 (2003) 654.

[22] F. Vidal, E. Farssac, J. Tusell, L. Puig, D. Gallardo, First molecular characterization of an unequal homologous Alu-mediated recombination event responsible for hemophilia, Thromb. Haemostasis 88 (2002) 12–16.

[23] C.J. Shaw, M.A. Withers, J.R. Lupski, Uncommon deletions of the Smith–Magenis syndrome region can be recurrent when alternate low-copy repeats act as homologous recombination substrates, Am. J. Hum. Genet. 75 (2004) 75–81.

[24] C. Lopez Correa, M. Dorschner, H. Brems, C. Lazaro, M. Clementi, M. Upadhyaya, D. Dooijes, U. Moog, H. Kehrer-Sawatzki, J.L. Rutkowski, J.P. Fryns, P. Marynen, K. Stephens, E. Legius, Recombination hotspot in *NF1* microdeletion patients, Hum. Mol. Genet. 10 (2001) 1387–1392.

[25] L. Fang, N. Chalhoub, W. Li, J. Feingold, J. Ortenberg, B. Lemieux, J.P. Thirion, Genotype analysis of the NF1 gene in the French Canadians from the Quebec population, Am. J. Med. Genet. 104 (2001) 189–198.

[26] L.J. Fang, D. Vidaud, M. Vidaud, J.P. Thirion, Identification and characterization of four novel large deletions in the human neurofibromatosis type 1 (NF1) gene, Hum. Mutat. 18 (2001) 549–550.

[27] R.A. Heim, L.N. Kam-Morgan, C.G. Binnie, D.D. Corns, M.C. Cayouette, R.A. Farber, A.S. Aylsworth, L.M. Silverman, M.C. Luce, Distribution of 13 truncating mutations in the neurofibromatosis 1 gene, Hum. Mol. Genet. 4 (1995) 975–981.

[28] C. Lazaro, A. Gaona, M. Lynch, H. Kruyer, A. Ravella, X. Estivill, Molecular characterization of the breakpoints of a 12-kb deletion in the NF1 gene in a family showing germ-line mosaicism, Am. J. Hum. Genet. 57 (1995) 1044–1049.

[29] L.M. Messiaen, T. Callens, G. Mortier, D. Beysen, I. Vandenbroucke, N. Van Roy, F. Speleman, A.D. Paepe, Exhaustive mutation analysis of the NF1 gene allows identification of 95% of mutations and reveals a high frequency of unusual splicing defects, Hum. Mutat. 15 (2000) 541–555.

[30] D. Viskochil, A.M. Buchberg, G. Xu, R.M. Cawthon, J. Stevens, R.K. Wolff, M. Culver, J.C. Carey, N.G. Copeland, N.A. Jenkins, et al., Deletions and a translocation interrupt a cloned gene at the Neurofibromatosis type 1 locus, Cell 62 (1990) 187–192.

[31] H. Kehrer-Sawatzki, J. Haussler, W. Krone, H. Bode, D.E. Jenne, K.U. Mehnert, U. Tummers, G. Assum, The second case of a t(17;22) in a family with neurofibromatosis type 1: sequence analysis of the breakpoint regions, Hum. Genet. 99 (1997) 237–247.

[32] H. Kurahashi, T. Shaikh, M. Takata, T. Toda, B.S. Emanuel, The constitutional t(17;22): another translocation mediated by palindromic AT-rich repeats, Am. J. Hum. Genet. 72 (2003) 733–738.

[33] R. Fahsold, T. Habash, U. Trautmann, A. Haustein, R.A. Pfeiffer, Familial reciprocal translocation t(17;19) (q11.2;q13.2) associated with neurofibromatosis type 1, including one patient with non-Hodgkin lymphoma and an additional t(14;20) in B lymphocytes, Hum. Genet. 96 (1995) 65–69.

[34] M.R. Wallace, L.B. Andersen, A.M. Saulino, P.E. Gregory, T.W. Glover, F.S. Collins, A de novo Alu insertion results in neurofibromatosis type 1, Nature 353 (1991) 864–866.

[35] C. Gervasini, A. Bentivegna, M. Venturin, L. Corrado, L. Larizza, P. Riva, Tandem duplication of the NF1 gene detected by high-resolution FISH in the 17q11.2 region, Hum. Genet. 110 (2002) 314–321.

[36] T. De Raedt, H. Brems, P. Wolkenstein, D. Vidaud, S. Pilotti, F. Perrone, V. Mautner, S. Frahm, R. Sciot, E. Legius, Elevated risk for

MPNST in NF1 microdeletion patients, Am. J. Hum. Genet. 72 (2003) 1288–1292.
[37] M. Venturin, P. Guanieri, F. Natacci, M. Stabile, R. Tenconi, M. Clementi, C. Hernandez, P. Thompson, M. Upadhyaya, L. Larizza, P. Riva, Mental retardation and cardiovascular malformations in NF1-microdeleted patients point to candidate genes in 17q11.2, J. Med. Genet. 41 (2004) 35–41.
[38] M. Clementi, S. Milani, I. Mammi, S. Boni, C. Monciotti, R. Tenconi, Neurofibromatosis type 1 growth charts, Am. J. Med. Genet. 87 (1999) 317–323.
[39] T. Haaf, D.C. Ward, Structural analysis of a-satellite DNA and centromere proteins using extended chromatin and chromosomes, Hum. Mol. Genet. 3 (1994) 697–709.
[40] N. Van Roy, G. Laureys, M. Van Gele, G. Opdenakker, R. Miura, P. van der Drift, A. Chan, R. Versteeg, F. Speleman, Analysis of 1;17 translocation breakpoints in neuroblastoma: implications for mapping of neuroblastoma genes, Eur. J. Cancer 33 (1997) 1974–1978.
[41] P. Lichter, T. Cremer, A practical approach, in: D.E. Rooney, B.H. Czipolkowski (Eds.), Human Cytogenetics, IRL Press, Oxford, 1992, pp. 157–192.